



## FTIR and electrical characterization of a-Si:H layers deposited by PECVD at different boron ratios

A. Orduña-Díaz<sup>a,\*</sup>, C.G. Treviño-Palacios<sup>a</sup>, M. Rojas-Lopez<sup>b</sup>, R. Delgado-Macuil<sup>b</sup>, V.L. Gayou<sup>b</sup>, A. Torres-Jacome<sup>a</sup>

<sup>a</sup> Instituto Nacional de Astrofísica, Óptica y Electrónica, Luís Enrique Erro No. 1, Tonantzintla, Puebla 72840, Mexico

<sup>b</sup> Centro de Investigación en Biotecnología Aplicada (CIBA), IPN, Tlaxcala, Tlax. 72197, Mexico

### ARTICLE INFO

#### Article history:

Received 1 September 2009

Received in revised form 8 April 2010

Accepted 25 April 2010

#### Keywords:

Hydrogenated amorphous silicon

Vibrational modes

PECVD

### ABSTRACT

Hydrogenated amorphous silicon (a-Si:H) has found applications in flat panel displays, photovoltaic solar cell and recently has been employed in boron doped microbolometer array. We have performed electrical and structural characterizations of a-Si:H layers prepared by plasma enhanced chemical vapor deposition (PECVD) method at 540 K on glass substrates at different diborane (B<sub>2</sub>H<sub>6</sub>) flow ratios (500, 250, 150 and 50 sccm). Fourier transform infrared spectroscopy (FTIR) measurements obtained by specular reflectance sampling mode, show Si–Si, B–O, Si–H, and Si–O vibrational modes (611, 1300, 2100 and 1100 cm<sup>-1</sup> respectively) with different strengths which are associated to hydrogen and boron content. The current–voltage curves show that at 250 sccm flow of boron the material shows the lowest resistivity, but for the 150 sccm boron flow it is obtained the highest temperature coefficient of resistance (TCR).

© 2010 Elsevier B.V. All rights reserved.

### 1. Introduction

Hydrogenated amorphous silicon was first studied during the 1950s and 1960s. One of the interesting properties of this material is its disordered structure and the presence of hydrogen which passivates the dangling bonds changing the structural morphology. When using boron as impurity improves not only the electrical and optical properties [1,2], but allow to tailor the properties of the deposited film for an specific application as in photodetectors [3], thin film transistors (TFTs) [4–6], solar cell fabrication [7,8] and array of microbolometers [9]. In these applications, the boron doping has to be optimized in order to meet the properties for which the amorphous semiconductor is going to be used. These properties are related to the carriers density, transport, generation and recombination such as dark conductivity, photoconductivity, density of gap states, mobility, lifetime [3,15]. Among the different methods for depositing hydrogenated amorphous silicon, we used plasma enhanced chemical vapor deposition [10] at low frequency. Our material (a-Si:H) is a semiconductor material in which the band structure is characterized by smooth variation of the density of states with energy in the band-edge zones, called band tails, and a high density of states in the midgap region. If the mobility of carriers in the band tails is high enough, the conduction mechanism is dominated by carriers activated from the midgap states to these

band tails. The conductivity of a-Si:H is usually thermally activated, at least over a limited temperature range and is described by Eq. (1).

$$\sigma(T) = \sigma_0 \exp\left(-\frac{E_a}{KT}\right) = \sigma_0 \exp\left[-\frac{E_{TR} - E_F}{KT}\right] \quad (1)$$

where  $\sigma$  is the conductivity,  $E_a$  is the activation energy,  $K$  is Boltzmann's constant,  $E_{TR}$  is defined as the average energy of the conducting electrons,  $\sigma_0$  is the conductivity prefactor,  $T$  is the temperature and  $E_F$  is the Fermi level.

We have analyzed the electric properties of layers of a-Si:H doped with different flows of diborane as a source of boron, while keeping constant all the other deposition parameters. The  $I$ – $V$  curves were used to determine conductivity and by observing the vibrational modes through FTIR reflectance measurements [11]; we correlate the presence of the different vibration associated to the various boron concentration and electrical properties observed for each case. This is relevant because in a PECVD deposited film, the resulting properties are not only function of the relative gas flow ratios of the reactants, but of all the depositing conditions, and a good figure of merit independent of the system like the vibrational modes. In this work the FTIR vibrational analysis is proposed as a reliable and fast tool for quantifying the desired properties adjustments of the B-doped a-Si:H.

### 2. Sample preparation

A set of a-Si:H films doped with boron (named samples A, B, C and D) were prepared in an AMP 3300 PECVD deposition system;

\* Corresponding author. Tel.: +52 248 4870765; fax: +52 224 84870766.

E-mail address: [abdu@susu.inaoep.mx](mailto:abdu@susu.inaoep.mx) (A. Orduña-Díaz).

**Table 1**  
Parameters for the deposition of B-doped a-Si:H by PECVD.

Samples	Power (W)	Frequency (kHz)	Temperature (K)	Time (min)	Flow of Ar (sccm)	Flow of SiH <sub>4</sub> (sccm)	Flow of B <sub>2</sub> H <sub>6</sub> (sccm)
A	300	110	540	30	100	50	500
B	300	110	540	30	100	50	250
C	300	110	540	30	100	50	150
D	300	110	540	30	100	50	50

it is a conventional capacitor coupled parallel-plate reactor. The RF frequency of the power supply was set at 110 kHz. All the films were deposited on glass substrates at a temperature of 540 K, the pressure was kept constant at 0.6 Torr. The reactive gases used were silane (SiH<sub>4</sub>) and argon (Ar) at a constant flow of 50 and 100 sccm respectively. Diborane was used as a boron source in a bottled 1% H<sub>2</sub> balanced gas mixture and the flow was varied in the range of 50–500 sccm. The a-Si:H layers thickness was measured by a stylus profilometer and the deposition time was adjusted to obtain a thickness of 120 nm approximately for all the films. The deposition parameters of the films are shown in Table 1. Al (1 μm thick) was evaporated on the surface of the deposited films and by using photolithography techniques electrodes were defined for electrical measurements.

**3. Sample characterization**

**3.1. Electrical characterization of the a-Si:H layers**

The resistance of the deposited films was measured in the 290–345 K temperature range through the I–V characteristics obtained from a Semiconductor Parameter Analyzer, and from these values the conductivity is calculated. Fig. 1 shows the behavior of the conductivity of the boron-doped films as a function of the reciprocal of temperature.

The activation energy can be estimated using Eq. (2), where σ is the conductivity.

$$\ln(\sigma) = -\frac{E_a}{KT} \quad (2)$$

Fig. 2 shows the dependence of ln(σ) as a function of 1/KT for the different diborane flows, in which the slope of the fitted line provides the activation energy (E<sub>a</sub>).

The temperature coefficient of resistance (TCR) is related to the activation energy as it is shown in Eq. (3).

$$TCR = -\frac{E_a}{KT^2} \quad (3)$$

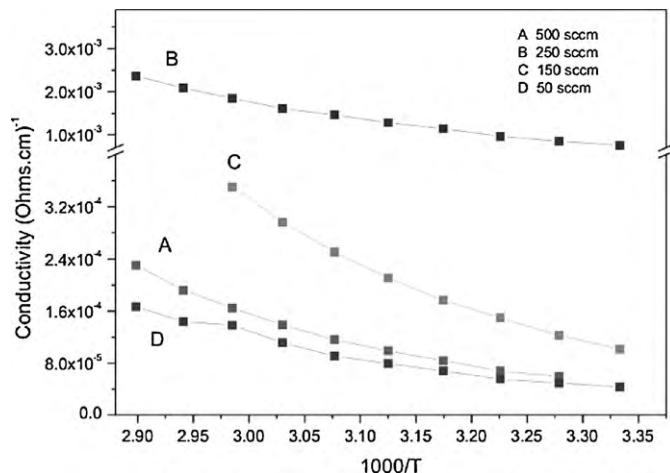


**Fig. 1.** Conductivity as a function of the inverse of the temperature for all the deposits.

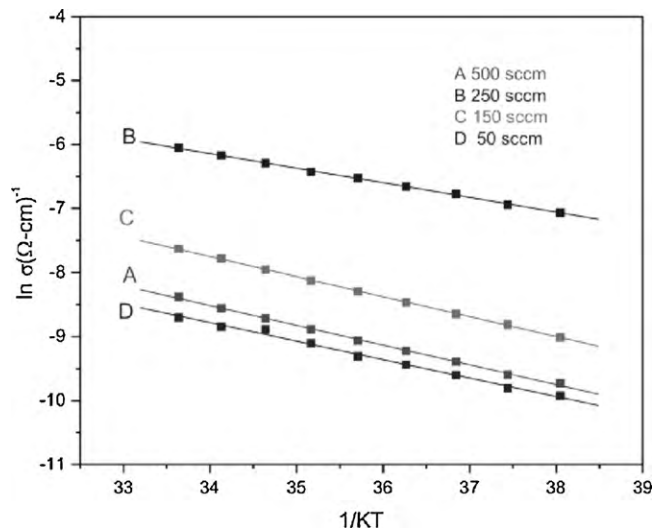


**Fig. 2.** Dependence of ln σ with 1/KT for the different concentration of diborane.

The conductivity at 300 K and the activation energy for all the samples is shown in Fig. 3. The inset shows the I–V curves for the set A of samples, showing a linear behavior of the deposited films. The dark conductivity increases from 50 to 250 sccm of diborane flux, after that, the dark conductivity begins to decrease. This is explained because as more dopant atoms are added to the films, they increase the coordination number defects, that for the deposition conditions here employed a flow greater than 250 sccm, generates more defects than electrically active dopants and therefore a reduction in conductivity is observed. An optimum flow of diborane is obtained in order to obtain the maximum conductivity in films in this deposition system. As is expected from Eq. (3), the activation energy has the minimum value when the film has the maximum dark conductivity. In Table 2 all this results are summarized.

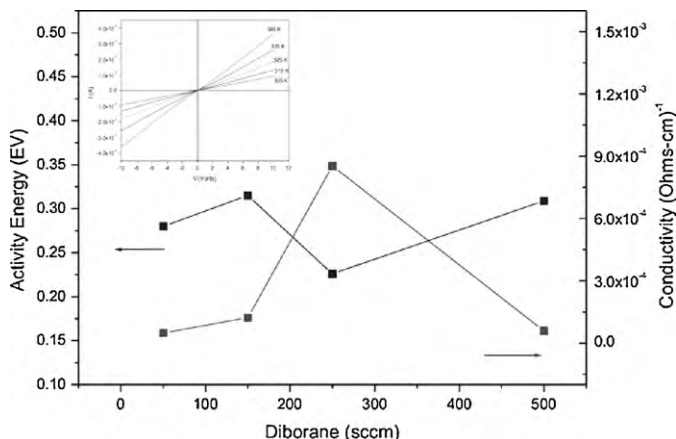


**Fig. 3.** Activation energy (E<sub>a</sub>) and conductivity σ for different flows of diborane.

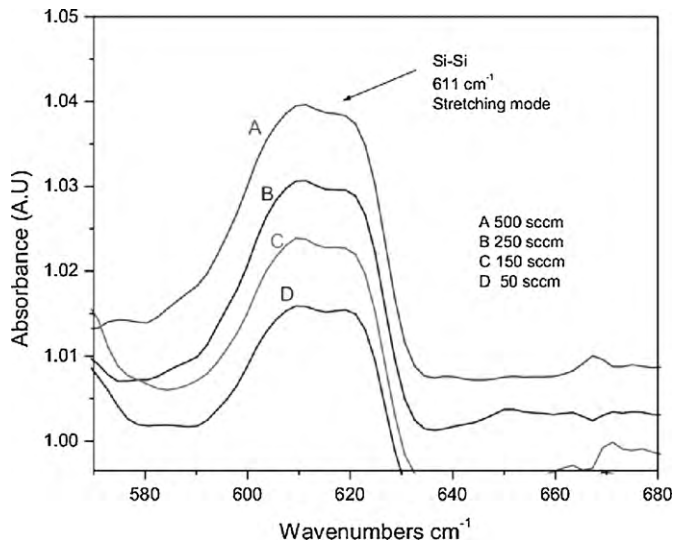


**Fig. 4.** Infrared spectra of layers at different boron ratios. The Si–Si vibrational mode is centered around  $611\text{ cm}^{-1}$ .

### 3.2. Vibrational analysis

The vibrational analysis was performed using a Fourier transform infrared spectrometer (FTIR) Bruker Vertex 70 in specular reflectance sampling mode. Fig. 4 shows the FTIR spectra of boron doped a-Si:H in the region of the Si–Si vibration mode, which has a well defined band at  $611\text{ cm}^{-1}$ . This band is associated to the transversal optical added to a transversal acoustic TO+TA vibrational mode of Si–Si bond arising from the monocrystalline silicon substrate (c-Si) [12]. This mode appears as the boron induces crystallization of the a-Si. In order to check this, Raman spectra were obtained for all the films and they are shown in Fig. 5.

As it can be seen in Fig. 5, the frequency of this band remains unchanged regardless of the boron flow [13], however the strength increases because of the layer become structurally more ordered according to Raman results shown in Fig. 5. The Raman spectra shows an intense band centered at  $521\text{ cm}^{-1}$  (longitudinal optical LO mode) arising from the c-Si induced at high boron fluxes, whereas for low boron fluxes the strength of this mode decreases because of the lack of crystallinity of the layer. Some other characteristic vibration modes of c-Si shown in Fig. 5 tend to disappear as the boron flux decreases. The band strengths are directly proportional to boron flux ratio, from 50 to 500 sccm. Fig. 6 shows the band of the B–O mode, which is close to  $1300\text{ cm}^{-1}$  and also increases its strength proportionally to the boron flux.

Figs. 7 and 8 show FTIR spectra in the Si–H and Si–O vibrational modes, which are located near  $2100$  and  $1100\text{ cm}^{-1}$  respectively. In this case, the peak strength enhance for each sample does not follow the boron flux ratio because the hydrogen plays a crucial role in damping the dangling bonds. This effect improves the electrical and optical properties by changes in the morphological structure [14]. As it is known on the deposition of a-Si:H, the hydrogen has an important role in the film network in which the hydrogen is bonded mainly in polyhydride configurations ( $\text{SiH}_3, \text{SiH}_2, \text{or} (\text{SiH}_2)_n$ ) [15],

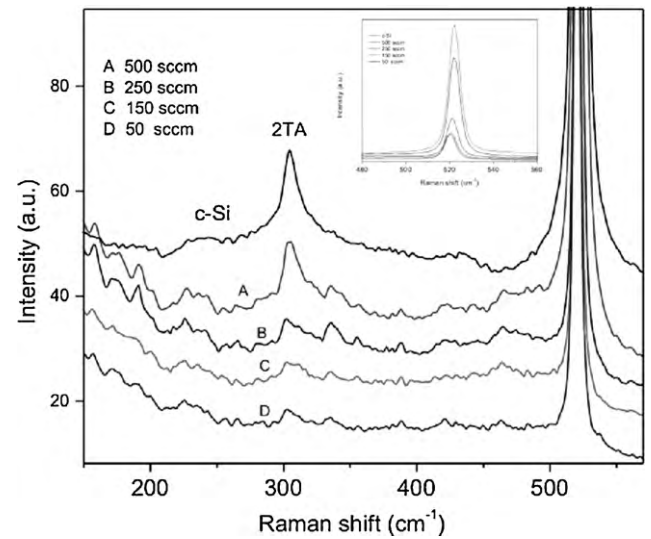


**Fig. 5.** Raman spectra of boron doped a-Si:H thin layers.

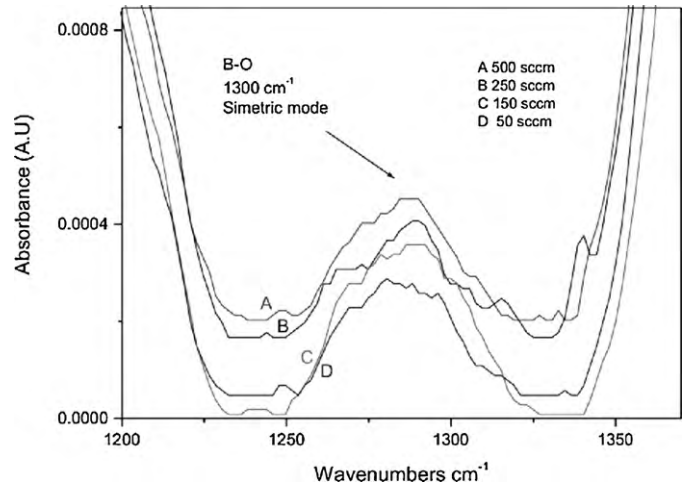


**Fig. 6.** The B–O vibrational mode near  $1300\text{ cm}^{-1}$ .

changing the thermal conductivity and the localized levels based on structural defects as well as the dependence of the band-edge energy (gap) on the content of bonded hydrogen. It can be seen that the sample with the lower resistivity (B), has the lowest Si–H bond content and also the lowest Si–O bond density. This relates very well with the observed electrical conductivity. This kind of bonds does not allow concluding about the other diborane flows used in this work. However the main conclusion of this study is that either the strength of the band at  $611\text{ cm}^{-1}$  or equivalently the Raman spectra are very useful in defining the best conductivity of the material, which in turn is related to the boron induced crystallinity effect.

The main vibration modes associated to the boron doped a-Si:H layers deposited by PECVD method are summarized in Table 3.

**Table 2**

Electrical properties of boron doped a-Si:H sample at 300 K.

Sample	Diborane	Activation energy, $E_a$ (eV)	Conductivity, $\sigma$ ( $\Omega\text{-cm}$ ) <sup>-1</sup>	Resistivity ( $\Omega\text{-cm}$ )	TCR <sup>a</sup> (%)
A	500	0.310	$5.95667 \times 10^{-5}$	16,787.9	3.98
B	250	0.229	$8.52148 \times 10^{-4}$	1173.5	2.91
C	150	0.310	$1.2261 \times 10^{-4}$	8155.9	4.06
D	50	0.288	$4.90555 \times 10^{-5}$	20,385.1	3.61

<sup>a</sup> Temperature coefficient of the resistance.

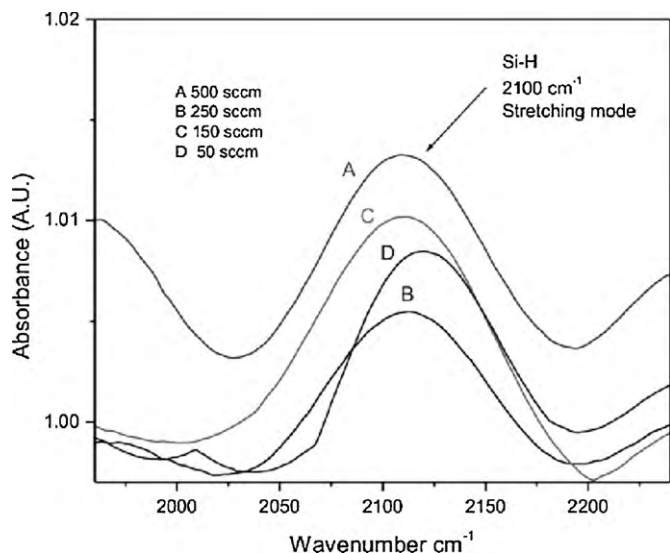


Fig. 7. Si-H vibrational mode at 2100  $\text{cm}^{-1}$ .

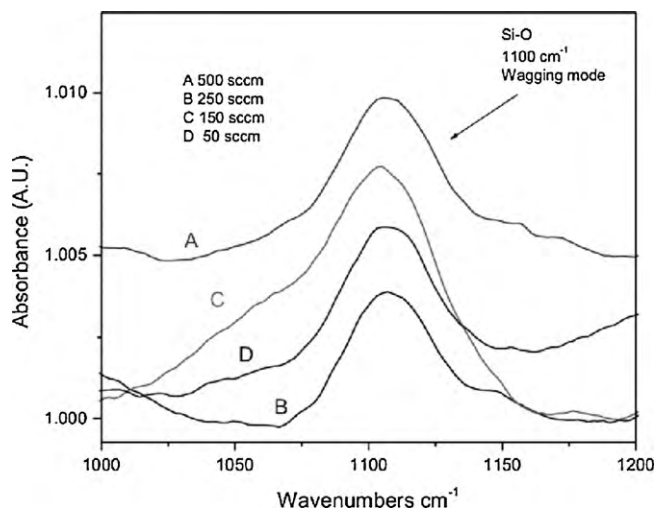


Fig. 8. Si-O vibrational mode at 1100  $\text{cm}^{-1}$ .

**Table 3**  
Vibration modes of boron doped a-Si:H layers.

Wavenumber ( $\text{cm}^{-1}$ )	Vibration mode	Reference
611	Si-Si Stretching	[16]
1100	Si-O Wagging	[17]
2100	Si-H Stretching	
1300	B-O Symmetric	[1]

#### 4. Conclusions

We have observed changes in boron doped a-Si:H films by changing the diborane flow during deposition, obtaining the optimal conditions for getting the best conductivity for transistor applications or the highest TCR as required for microbolometer construction using the B-doped a-Si:H as the thermo-sensing material. It was found that for our deposition system and conditions, a 250 sccm boron flow is the best for obtaining the lowest resistivity of the material. The highest TCR value obtained is found at a flow of 150 sccm of diborane, which is appropriate for microbolometer construction. Important structural changes based on the hydrogen and boron content was observed by FTIR associated to hydrogen and boron content was identified on vibrational modes, accordingly to the possible application.

#### Acknowledgments

This work was partially supported by CONACYT-SALUD-2005-01-14012 grant. A. Orduña-Díaz thanks CONACYT for granting him a Ph.D. scholarship.

#### References

- [1] D.L. Flamm, Plasma chemistry basic processes and PECVD, in: P.F. Williams (Ed.), Plasma Processing of Semiconductors, Kluwer Academic Publishers, 1997, p. 34.
- [2] G.R. Yang, Y.P. Zhao, B.Y. Tong, J. Vac. Sci. Technol. A 16 (4) (1997) 2267–3371.
- [3] J.P.M. Schmitt, J. Non-Cryst. Solids 59–60 (1983) 649–657.
- [4] S. Sedky, P. Fiorini, M. Caymax, S. Loreti, K. Baert, L. Hermans, R. Mertens, J. Microelectromech. Syst. 7 (4) (1998) 365–371.
- [5] W. Luft, Y.S. Tsuo, Hydrogenated Amorphous Silicon Allow Deposition Processes, Dekker, New York, 1993.
- [6] S.S. He, M.J. Williams, D.J. Stephens, G. Lucovsky, J. Non-Cryst. Solids 52 (1993) 164–166.
- [7] K. Yamamoto, M. Yoshimi, Y. Tawada, Y. Okamoto, A. Nakajima, S. Igari, Appl. Phys. A 69 (1999) 179–185.
- [8] B.P. Nelson, E. Iwaniczko, A. Harv Mahan, Qi Wang, Yueqin Xu, R.S. Crandall, H.M. Branz, Thin Solid Films 395 (2001) 292–297.
- [9] A. Heredia-J, A. Torres-J, J. De la Hidalga-W, A. Jaramillo-N, Mater. Res. Soc. Symp. Proc. 744 (2003), M5.26.1–M5.26.6.
- [10] M. Moravej, S.E. Babayan, G.R. Nowling, X. Yang, R.F. Hicks, Plasma Sources Sci. Technol. 13 (2004) 8–14.
- [11] M.H. Brodsky, M. Cardona, J.J. Cuomo, Phys. Rev. B 16 (1977) 3556–3571.
- [12] R. Boyle, Application Note: 50640, FTIR Measurement of Interstitial Oxygen and Substitutional Carbon in Silicon Wafers, Thermo Fisher Scientific, Madison, WI, USA, 2008.
- [13] R. Saleh, N.H. Nickel, Thin Solid Films 427 (2003) 266–269.
- [14] H. Okamoto, Optical and Electrical Properties, in: K. Tanaka, E. Maruyama, T. Shimada, H. Okamoto (Eds.), Amorphous Silicon, first ed., John Wiley and Sons, Tokyo, Japan, 1993, pp. 103–179.
- [15] K. Tanaka, Methods of preparation and growth processes, in: K. Tanaka, E. Maruyama, T. Shimada, H. Okamoto (Eds.), Amorphous Silicon, first ed., John Wiley and Sons, Tokyo, Japan, 1993, pp. 27–56.
- [16] M.A. Vasquez, G. Aguilar Rodríguez, G. García Salgado, G. Romero-Paredes, R. Peña-Sierra, Revista Mexicana de Física 53 (6) (2007) 431–435.
- [17] L. Gedvilas, B. Keyes, T. Ciszek, G. Jorgensen, B. Nelson, Y. Xu, J. Perkins, The National Center for Photovoltaics and Solar Program Review Meeting, 2003, pp. 1–3.